Truncation of GalNAc-type O-glycans Suppresses CD44-mediated Osteoclastogenesis and Bone Metastasis in Breast Cancer

Neng-Yu Lin[1], Jian-Jr Lee[2,3], Syue-Ting Chen[1,4], Jung-An Lin[1], Chia-Hsuan Lin[1], Hsuan-Yu Lin[1], Yong-Han Su[5], Cheng-Chang Chen[5,6], Mei-Chun Lin[7], Ching-Ying Kuo[5,6], and Min-Chuan Huang[1]

ABSTRACT

The glycoprotein CD44 is a key regulator of malignant behaviors in breast cancer cells. To date, hyaluronic acid (HA)-CD44 signaling pathway has been widely documented in the context of metastatic bone diseases. Core 1 β1,3-galactosyltransferase (C1GALT1) is a critical enzyme responsible for the elongation of O-glycosylation. Aberrant O-glycans is recognized as a hallmark in cancers. However, the effects of C1GALT1 on CD44 signaling and bone metastasis remain unclear. In this study, IHC analysis indicated that C1GALT1 expression positively correlates with CD44 in breast cancer. Silencing C1GALT1 accumulates the Tn antigen on CD44, which decreases CD44 levels and osteoclastogenic signaling. Mutations in the O-glycosites on the stem region of CD44 impair its surface localization as well as suppress cell–HA adhesion and osteoclastogenic effects of breast cancer cells. Furthermore, *in vivo* experiments demonstrated the inhibitory effect of silencing C1GALT1 on breast cancer bone metastasis and bone loss. In conclusion, our study highlights the importance of O-glycans in promoting CD44-mediated tumorigenic signals and indicates a novel function of C1GALT1 in driving breast cancer bone metastasis.

Implications: Truncation of GalNAc-type O-glycans by silencing C1GALT1 suppresses CD44-mediated osteoclastogenesis and bone metastasis in breast cancer. Targeting the O-glycans on CD44 may serve as a potential therapeutic target for blocking cancer bone metastasis.

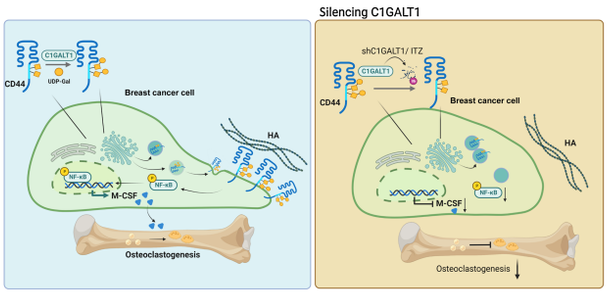

Introduction

Bone metastases frequently occur in almost all tumors, especially in 65% to 75% of patients with breast cancer. This high incidence rate has become the leading cause of cancer-related deaths worldwide (1). Bone metastatic breast cancer is mainly due to osteolytic bone destruction and systemic bone loss by triggering osteoclastogenesis (2). Increasing evidence suggests that breast cancer bone metastasis is relevant to cancer cell–mediated elevation of activators such as Interleukin-1 β (IL1b), Interleukin 6 (IL6), macrophage colony stimulating factor (M-CSF) receptor activator of nuclear factor kappa-B ligand (RANKL), and CD44 signaling, which activate osteoclasts and disrupt the homeostatic balance of bone formation and degradation (3–9). Particularly, the serum levels of M-CSF, the essential activator of osteoclastogenesis, were significantly higher in patients with bone metastatic cancer than in patients with nonmetastatic (10). The regulatory factors of bone metastasis and mechanisms of osteoclastogenesis driven by metastatic breast cancer cells are highly glycosylated. However, the function of glycosylation in breast cancer bone metastasis and cancer cell–mediated bone loss is still poorly understood.

Glycosylation is the most common co/posttranslational modification of proteins, which is frequently altered during tumor progression (11). Core 1 β1,3-galactosyltransferase 1 (C1GALT1) transfers galactose from uridine diphosphoglucose (UDP)-galactose to the Tn antigen (GalNAc-α-Ser/Thr), forming the core 1 structure (Gal-β1,3-GalNAc-α-Ser/Thr), which is the precursor for the biosynthesis of more complex O-glycans (12). The core 1 structure, also known as Thomsen–Friedenreich antigen, has been demonstrated as a pan-carcinoma antigen and a surface marker of disseminated tumor cells in the bone marrow of patients with breast cancer for decades (13, 14). Previous studies have consistently reported that C1GALT1 is enriched in many types of cancer, such as hepatocellular carcinoma (HCC), gastric adenocarcinoma, colorectal adenocarcinoma, prostate cancer, breast adenocarcinoma,

[1]Graduate Institute of Anatomy and Cell Biology, College of Medicine, National Taiwan University, Taipei, Taiwan. [2]Department of Plastic and Reconstructive Surgery, China Medical University Hospital, Taichung, Taiwan. [3]School of Medicine, China Medical University, Taichung City, Taiwan. [4]Department of Anatomy, Graduate Institute of Biomedical Sciences, College of Medicine, Chang Gung University, Taoyuan, Taiwan. [5]Department of Clinical Laboratory Sciences and Medical Biotechnology, College of Medicine, National Taiwan University, Taipei, Taiwan. [6]Department of Laboratory Medicine, National Taiwan University Hospital, Taipei, Taiwan. [7]Department of Otolaryngology, National Taiwan University Hospital, Taipei, Taiwan.

Corresponding Author: Neng-Yu Lin, Graduate Institute of Anatomy and Cell Biology, College of Medicine, National Taiwan University, Taipei 100, Taiwan. Phone: 8862-2312-3456, ext. 288179; Fax: 8862-2391-5292; E-mail: nylin@ntu.edu.tw

Mol Cancer Res 2023;21:664–74

doi: 10.1158/1541-7786.MCR-22-0907

and head and neck cancer. Moreover, suppressing the signaling of mucin 1 (MUC1) and receptor tyrosine kinases (RTK) by disrupting core 1–mediated O-glycosylation has been intensively reported to impair tumor cell malignant properties (15–22). Notably, CD44, the main receptor for hyaluronan, is a highly O-glycosylated protein in breast cancer cells. Compared with standard CD44 (CD44s), variant (CD44v) isoforms of CD44 have been shown to be created by alternative RNA splicing in several metastatic cancers (23–26). Changes in HA-binding affinity and the recruitment of CD44 to the cell surface have been investigated using CD44 with variable N and O-linked glycosylation (27–29). However, contradictory results were obtained by the different groups due to the different cell types and experimental approaches used. Further investigation of CD44 glycoproteins harboring aberrant O-glycosylation, that is, formation of Tn and sialyl-Tn structures, to influence breast cancer bone metastasis is warranted.

In this study, we aimed to elucidate the effect of Tn antigen expression on cancer cell–mediated osteoclastogenesis and bone metastasis by targeting CD44 O-glycosylation in breast cancer. Here, we applied genetic and pharmacologic approaches to enrich glycoproteins with Tn-antigens in breast cancer cell lines; CD44 was the dominant Tn-carrying protein pulled down by GalNAc-binding lectin. Tn-antigen–expressing CD44 was found to impair its translocation at plasma membrane and breast cancer cell-mediated osteoclast differentiation. In addition, similar properties were observed in breast cancer cells expressing multiple O-glycosylation site mutants of CD44. Our findings indicated that C1GALT1-mediated glycosylation contributes to breast cancer bone metastatic properties by regulating CD44 signaling.

Materials and Methods

IHC

Paraffin-embedded breast cancer tissue microarray (BR1141) was obtained from US Biomax Inc. for IHC staining. Decalcified, paraffin-embedded tibial bones from mock and shC1GALT1 MDA-MB-231 cell–injected mouse groups were cut into 5-μm sections for IHC staining. Monoclonal anti-C1GALT1 (Santa Cruz Biotechnology, sc-100745), anti-CD44 (Invitrogen, IM7, that reacts with all isoforms of CD44), and polyclonal anti-M-CSF (GeneTex, GTX81735) antibodies were used and detected with Super Sensitive Link-Label IHC Detection System (BioGenex). The specific staining was visualized with a 3,3-diaminobenzidine liquid substrate system (Sigma) and counterstained with hematoxylin (Sigma). Tissue sections were examined and scored by two independent investigators blinded to the clinicopathologic data.

Plasmid construction

Full-length human CD44 (accession number BC004372) was subcloned into pCDH-EF1-MCS-T2A-Puro (a gift from Dr. Kuo's lab), labeled CD44 wild type (Wt). GalNAc-type O-glycosylation mutant of CD44 with multiple mutations at O-glycosylation sites of CD44 (from a.a. 416–638, 38 identified S/Ts were mutated into A, SF2), labeled CD44 Mu. The mutated DNA fragment was generated and sequenced by commercial services (IDT).

Cell lines and cell culture

MDA-MB-231, MDA-MB-436, and MCF-7 cells were purchased from Bioresource Collection and Research Centre (BCRC, Taiwan). All cell lines were authenticated using short tandem repeat (STR) profiling analysis. Cells were cultured in DMEM(Invitrogen) containing 10% FBS (Invitrogen), 100 IU/mL penicillin, and 100 μg/mL streptomycin (Invitrogen) in a humidified cell culture incubator at 37°C in a 5% CO_2 atmosphere. The C1GALT1-specific inhibitor, itraconazole (Sigma), was applied to the culture medium at a final concentration of 2.5 μmol/L and incubated for 3 days. All cells were tested for *Mycoplasma* contamination every 3 months during culture as routine test using Mycoplasma Detection Kit (D101, Vazyme Biotech Co., Ltd) to ensure that the cells were *Mycoplasma* free. For stable knockdown of C1GALT1 and CD44 in breast cancer cells, sh-C1GALT1/pLKO.1-puro, sh-CD44/pLKO.1-puro, and sh-Ctrl/pLKO.1-puro (RNAi Core, Academia Sinica) were used in a lentivirus-based infection system, and stable pooled clones were selected and maintained with 1 μg/mL puromycin (Sigma). The following target sequences were used: shC1GALT1 (5′ CCCAGCCTAATGTTCTTCATA 3′) and shCD44 (5′ CCTCCCAGTATGACACATATT 3′). For stable overexpression of C1GALT1, CD44 Wt, and CD44 Mu in MCF-7 cells, C1GALT1/pCDH-EF1-MCS-T2A-Puro, CD44 Wt/pCDH-EF1-MCS-T2A-Puro, and CD44 Mu/pCDH-EF1-MCS-T2A-Puro were used in lentivirus-based infection system, and stable pooled clones were selected and maintained with 1 μg/mL puromycin (Sigma).

Cell–HA adhesion assay

Twenty-four–well culture plates were coated with 5 mg/mL HA in carbonate-bicarbonate coating buffer, pH 7.5, for 18 hours at 4°C. Plates were washed with PBS containing 0.05% Tween 20 and blocked with 1% BSA for 3 hours at room temperature. Breast cancer cells from each group were seeded at a density of 1×10^5 cells/well to adhere for 10 minutes at 37°C, after which wells were carefully washed with PBS to remove nonadherent cells. Adherent cells were photographed and counted for analysis.

Osteoclast differentiation assay

Donor mice were sacrificed at the age of 4 weeks. Bone marrow cells from the tibia and femur were flushed with PBS. The cells were cultured in conditioned medium supplemented with 5 ng/mL RANKL (R&D Systems) for three days. Osteoclast differentiation was evaluated by staining cells for tartrate-resistant acid phosphatase (TRAP) using a Leukocyte Acid Phosphatase Kit (Sigma-Aldrich). TRAP-positive multinucleated cells (more than three nuclei) were counted under a phase-contrast microscope for statistical analysis.

Flow cytometry

For detection of CD44 antigens on cell surfaces, cells (1×10^5) were resuspended in 100 μL PBS with 0.5% BSA, pretreated with neuraminidase (Sigma), and incubated with CD44-FITC (Invitrogen) at 1:100 in PBS with 0.5% BSA. After washing twice, the fluorescence intensity of 10,000 cells per sample in 100 μL PBS was analyzed by flow cytometry (FACSCalibur; BD Pharmingen). Samples with control serum-binding served as negative controls. Experimental results were obtained from three independent replications.

Western blot analysis and lectin pull-down assay

Cell lysates were extracted in lysis buffer (Thermo Fisher Scientific). Proteins were separated by 10% SDS-PAGE and transferred onto polyvinylidene difluoride (PVDF) membranes. The membranes were blocked in TBST containing 5% BSA (Bio-Rad) and then incubated with mAbs against GAPDH (Santa Cruz Biotechnology), C1GALT1 (Santa Cruz Biotechnology), CD44 (Invitrogen), phospho-NF-κB p65 (Ser536), and NF-κB p65 (Cell Signaling Technology),

polyclonal antibodies against M-CSF (GeneTex), and biotinylated Vicia villosa (VVA) lectins (Vector Laboratories). After incubation with horseradish peroxidase (HRP)-conjugated secondary antibodies and HRP-conjugated streptavidin, protein bands were detected with enhanced chemiluminescence (ECL) reagents (GE Healthcare Life Sciences). For the lectin pull-down assay, 500 μg of total proteins from cell lysates with or without 0.4 U/mL neuraminidase (Sigma-Aldrich) treatment were incubated with VVA lectin–conjugated beads (Vector Laboratories). The beads were washed and boiled to pull down proteins. The samples were separated by SDS-PAGE for Western blot analysis and MS analysis. Experimental results were obtained from three independent replications.

Immunofluorescence staining

Cells were cultured in chamber slides (SPL Life Sciences), fixed with 4% paraformaldehyde (PFA), permeabilized with 0.25% Triton X100, blocked in PBS containing 2% BSA (Bio-Rad), and incubated with primary antibodies against CD44 (Invitrogen). Alexa Fluor antibodies (Life Technologies) were used as secondary antibodies. Isotype control antibodies were used as controls. Cell nuclei were visualized with 4',6-diamidino-2-phenylindole (DAPI; Santa Cruz Biotechnology). Images were randomly captured using a Leica TCS - SP5 fluorescence microscope (Major Instruments Co., Ltd.).

Animals

All animal experiments were approved by the Institutional Animal Care and Use Committee (IACUC) of National Taiwan University College of Medicine, Taipei, Taiwan. Female NOD/SCID mice (8 mice per group) aged six weeks were purchased from the National Laboratory Animal Center, Taipei, Taiwan. For experimental metastasis analysis, MDA-MB-231 cells (mock and shC1GALT1, 5×10^6) were intracardially injected into the ventricles of mice. Animals were sacrificed on day 60 for evaluation of bone metastasis.

Micro-CT analysis

Mouse tibia bones were analyzed by micro-CT (SkyScan 1076; SkyScan n.v.). The following acquisition parameters were used: voltage: 50 kV; X-ray current: 200 mA; exposure time: 500 ms/projection, 720 projections; matrix: 1024×1024; and voxel size in the reconstructed image: 9 μm. The micro-CT images were imported into CTAn software (Skyscan) to measure the four parameters of trabecular bone microarchitecture: BV/TV, Tb. Th., Tb. Sp., and Tb. N. of the cancellous bone in the proximal metaphysis of the tibia bone.

Histomorphometric analysis

Decalcified, paraffin-embedded tibial bones were cut into 5-μm sections and stained with hematoxylin & eosin (H&E; Merck) or TRAP using a leukocyte acid phosphatase staining kit (Sigma-Aldrich). The bone metastasis area and osteoclast number were analyzed with ImageJ.

Statistical analysis

All data are expressed as the mean ± SEM. Statistical analyses were performed using Student *t* tests or nonparametric Mann–Whitney U tests (for RT-qPCR, TRAP staining, cell adhesion analyses, and IHC analyses). One-way ANOVA followed by Dunnett multiple comparisons test was used to analyze multiple experimental groups. Correlation analyses were performed using the Pearson rank-sum test. *P* values of less than 0.05 were considered statistically significant; *P* values are expressed as follows: $0.05 > P > 0.01$ as *; $0.01 > P > 0.001$ as **; $P < 0.001$ as ***.

Data availability

The data generated in this study are available upon request from the corresponding author.

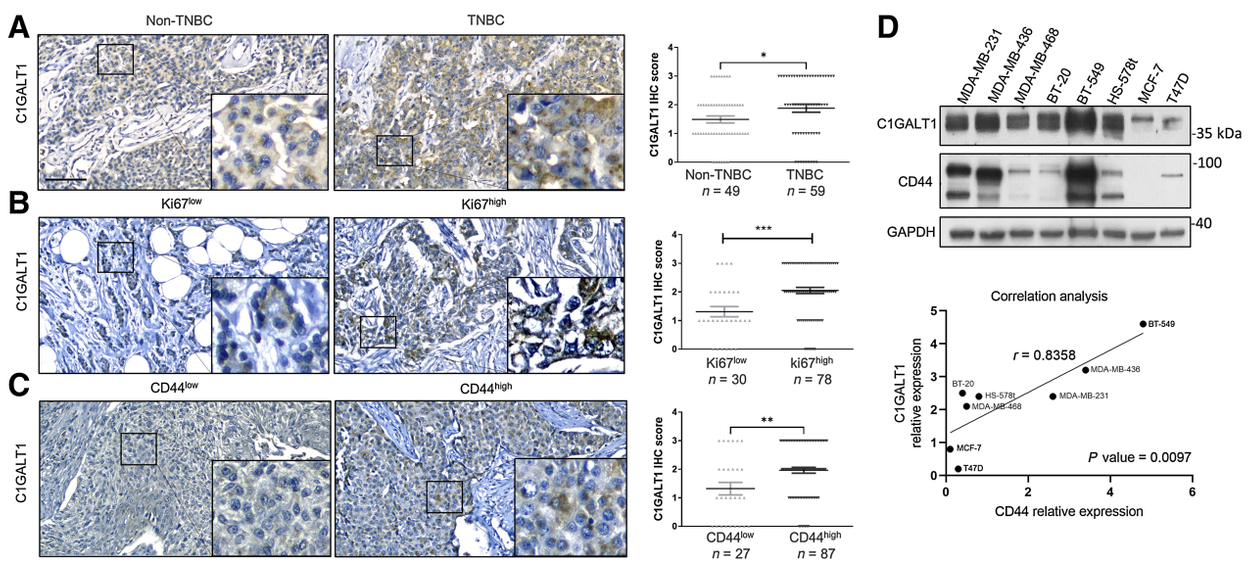

Figure 1.

C1GALT1 is highly expressed in triple-negative and Ki67^{high} breast cancer. **A,** Representative IHC staining of C1GALT1 in nontriple-negative and TNBC. Scale bar, 100 μm. **B,** Representative IHC staining of C1GALT1 in Ki67^{low} and Ki67^{high} breast tumor tissues. **C,** Representative IHC staining of C1GALT1 in CD44^{low} and CD44^{high} breast tumor tissues. The staining intensity of C1GALT1 was scored from 0, +1, +2, and +3 and is graphed against TNBC, Ki67, and CD44 markers in **A–C,** respectively. *N* indicates the number of patients. **D,** Immunoblotting analysis of CD44 and C1GALT1 expression in various triple negative and non–triple-negative breast cancer cell lines, using GAPDH as an internal control. Bottom, Pearson correlation analysis of C1GALT1 and CD44 protein expression. ($r = 0.836$, $P < 0.01$).

Results

C1GALT1 is highly expressed in triple-negative and Ki67–high breast cancer

We previously reported that C1GALT1 protein is overexpressed in breast cancer tissues compared with normal tissues and correlates with advanced tumor stages (19). We further analyzed the expression levels of C1GALT1 in a tissue array containing 114 human breast tumors with known clinicopathologic markers (estrogen receptor; ER, partial response; PR, HER2, and Ki67). The IHC staining intensity of C1GALT1 was scored into four categories: "−" (no stained cells or only isolated single stained cells), "1+" (weak expression, approximately 25% of cells stained), "2+" (moderate expression, ∼ 25%–75% of cells stained) and "3+" (strong expression, more than 75% of cells stained). We found that tumors from patients with triple-negative breast cancer (TNBC) expressed higher levels of C1GALT1 than those from patients with nonTNBC (**Fig. 1A**; **Table 1**). In addition, higher expression (immunoreactivity 2+ to 3+) of C1GALT1 was detected in Ki67-high tumors than in Ki67-low tumors (**Fig. 1B**; **Table 1**). Moreover, the statistical results indicated that high C1GALT1 expression was found in 71.2% (42/59) of TNBC tumors and in 70.5% (55/78) of Ki67-high tumors (**Table 1**). These results suggest that C1GALT1 is highly expressed in triple-negative and Ki67 high–expressing breast cancer.

Table 1. Correlation between C1GALT1 expression and clinicopathologic parameters in patients with breast cancer.

Breast cancer ($N = 114$)				
	C1GALT1 intensity			
Characteristics	**Low**	**High**	**Total**	***P***
Age (years)	—	—	—	0.460
≤50	28	41	69	—
>50	17	28	45	—
Tumor size	—	—	—	0.564
T1–2	35	54	89	—
T3–4	10	15	25	—
Lymph node metastasis	—	—	—	**0.015***
No	36	40	76	—
Yes	9	29	38	—
Stage	—	—	—	0.385
I & IIA	26	43	69	—
IIB & IIIA	19	26	45	—
ER	—	—	—	0.570
Negative	34	53	87	—
Positive	8	13	21	—
PR	—	—	—	0.534
Negative	37	59	96	—
Positive	5	7	12	—
HER2	—	—	—	0.392
Negative	33	49	82	—
Positive	9	17	26	—
Triple-negative	—	—	—	**0.0184***
No	25	24	49	—
Yes	17	42	59	—
Ki67	—	—	—	**0.001****
Low	19	11	30	—
High	23	55	78	—
CD44	—	—	—	**0.016***
Low	16	11	27	—
High	29	58	87	—

Note: *, $P < 0.05$; **, $P < 0.01$.

Expression of C1GALT1 correlates with CD44 in breast cancer

C1GALT1 is highly correlated with the expression of Ki67, that has been reported to be associated with bone metastases in patients with breast cancer (30). Therefore, we hypothesized that C1GALT1 could promote breast cancer bone metastasis. CD44 expression is particularly relevant in bone metastatic breast cancer, as its enrichment results in poor prognosis and shorter skeletal disease-free survival (31). To investigate the correlation of C1GALT1 and CD44 expression, the IHC staining intensity of C1GALT1 and CD44 in the breast cancer tissue arrays was scored from 0 to +3 and divided into low (scores 0 and 1) and high (scores 2 and 3) groups. The results showed that C1GALT1 expression was positively associated with CD44 expression in breast tumors (**Fig. 1C**; **Table 1**). C1GALT1 and CD44 expression in a panel of breast cancer cell lines were analyzed using Western blot analysis to validate the correlation. Pearson correlation analysis showed that C1GALT1 expression was positively correlated with CD44 protein expression ($r = 0.836$, $P < 0.001$), as shown in the bottom panel (**Fig. 1D**). Our results confirmed high expression of C1GALT1 and CD44 in TNBC cell lines and the positive correlation between C1GALT1 and CD44 expression.

Downregulation of C1GALT1 inhibits the hyaluronic acid binding and cancer-associated osteoclast differentiation of breast cancer cells *in vitro*

The modification of N-glycosylation sites of CD44 led to distinct hyaluronic acid (HA)-binding properties in different cancers (32, 33). However, the effect of cell surface GalNAc-type O-glycans on HA-binding to breast cancer cells has not yet been thoroughly investigated. CD44 possesses the properties of the primary receptor for HA and is a heavily O-glycosylated membrane receptor in cells, which is a reasonably viable target to elucidate the effect of GalNAc O-glycans on HA binding (34). First, we performed Western blot analyses to confirm the knockdown of C1GALT1 and CD44 in breast cancer cells. Interestingly, we found that downregulation of C1GALT1 decreased CD44 protein levels without a significant change in its mRNA level (**Fig. 2A**; Supplementary Fig. S1). Cell–HA adhesion assays were performed to examine the effect of C1GALT1-mediated O-glycosylation on CD44-HA interaction. The results showed that C1GALT1 knockdown inhibited breast cancer cell adhesion to HA, that was phenocopied by CD44 knockdown (**Fig. 2B**), suggesting that C1GALT1-mediated O-glycosylation is involved in CD44–HA interaction. The CD44–HA interaction in bone metastasis and cancer-associated osteoclast differentiation has recently attracted considerable interest. Murine bone marrow mononuclear cells (BMMC) were treated with the conditioned medium of MDA-MB-231 or MDA-MB-436 cells in combination with RANKL to elucidate the effect of Tn antigen expression on cancer cell–mediated osteoclast differentiation. TRAP staining showed that the conditioned media from C1GALT1 and CD44 knockdown breast cancer cells significantly prevented osteoclast differentiation (**Fig. 2C**). These results suggest that silencing C1GALT1 inhibits HA-binding to breast cancer cells and suppresses breast cancer-associated osteoclast differentiation *in vitro*.

Impacts of C1GALT1-mediated O-glycans on the surface expression of CD44 and osteoclastogenic signaling

Several studies have identified the essential function of C1GALT1-mediated O-glycosylation in activating RTKs, such as EGFR and EPHA2, and regulating the surface localization, such as TrkA, that are involved in cancer progression and metastasis (15, 18, 35). However, the effects of C1GALT1-mediated O-glycans on CD44, a non-kinase cell surface transmembrane glycoprotein, have remained

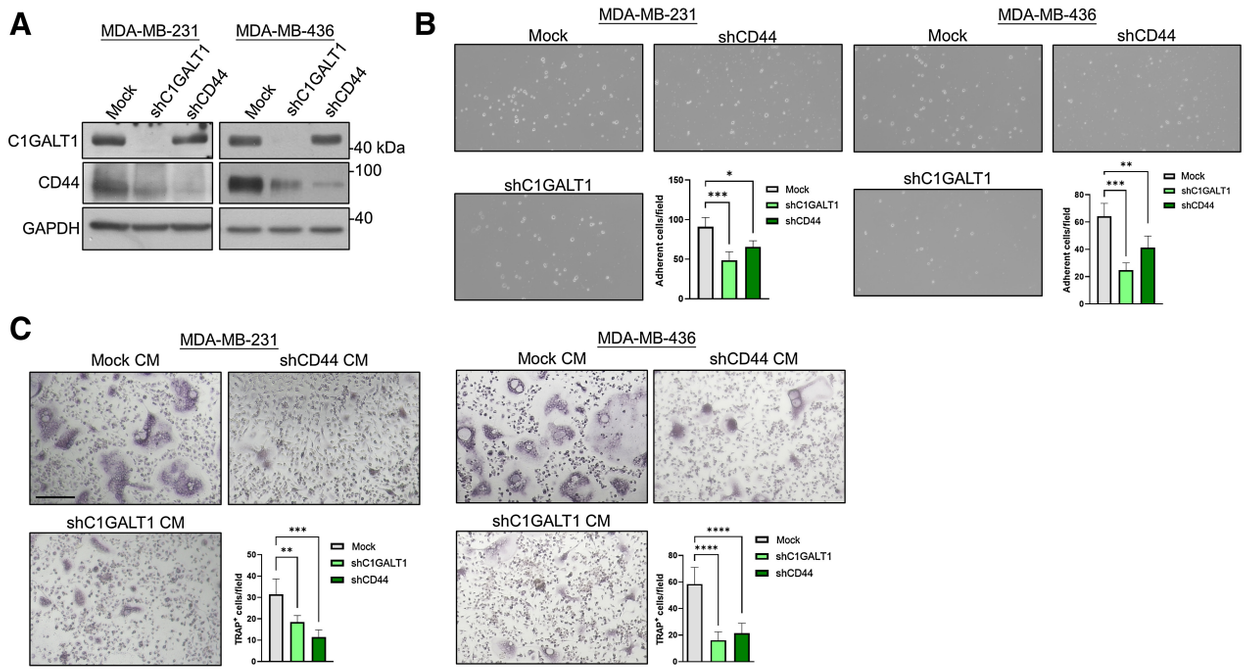

Figure 2.

Downregulation of C1GALT1 in breast cancer cells inhibits the HA binding and cancer-associated osteoclast differentiation. **A,** Knockdown of C1GALT1 or CD44 in MDA-MB-231 and MDA-MB-436 cells. Cells were transfected with sh-Ctrl/pLKO.1-puro (mock), sh-C1GALT1/pLKO.1-puro against C1GALT1 (shC1GALT1), or sh-CD44/pLKO.1-puro against CD44 (shCD44) for 48 hours and analyzed using Western blotting analysis. GAPDH was used as an internal control. **B,** Adhesion of breast cancer cells to immobilized HA. Representative images of breast cancer cells adhered to HA-coated plates were shown. Data are presented as the mean ± SD ($n = 3$). *, $P < 0.05$; **, $P < 0.01$; ***, $P < 0.001$. **C,** Effects of C1GALT1 or CD44 knockdown in breast cancer cells on osteoclast differentiation. Representative images showing TRAP staining of *in vitro* differentiated osteoclasts derived from mouse bone marrow cells treated with conditioned medium (CM) from mock, C1GALT1-knockdown, or CD44-knockdown breast cancer cells. Data are presented as the mean ± SD of TRAP-positive cells ($n = 3$). Scale bar, 100 μm. *, $P < 0.05$; **, $P < 0.01$; ***, $P < 0.001$; ****, $P < 0.0001$.

unclear in breast cancer. Many CD44 functions are associated with its ability to interact with HA, and this ability can be further regulated by several mechanisms, including surface levels of CD44. Therefore, the regulatory mechanisms of targeting CD44 to the cell surface need to be clarified. We performed immunofluorescence (IF) staining to detect the localization of CD44 in C1GALT1 knockdown or overexpressing breast cancer cells cultured in HA-coated chamber slides. The results from confocal microscopy demonstrated that CD44 was predominantly localized on the focal adhesion in control cells; however, CD44 was limited to the intracellular vesicles in C1GALT1 knockdown cells. To confirm the effect of C1GALT1 on subcellular localization of CD44, C1GALT1 was overexpressed in MCF-7 cells, that are CD44 low-expressing breast cancer cells. Consistently, CD44 was dramatically increased on focal adhesions in C1GALT1-overexpressing MCF-7 cells (**Fig. 3A**). In line with this finding, flow cytometry showed that silencing C1GALT1 decreased the surface levels of CD44 on MDA-MB-231 and MDA-MB-436 cells. In contrast, the surface levels of CD44 were increased on C1GALT1-overexpressing MCF-7 cells (**Fig. 3B**).

HA–CD44 interaction activates several signaling pathways responsible for the malignant phenotypes of breast cancer cells. Therefore, we tested whether the altered O-glycans on CD44 by C1GALT1 knockdown affect its downstream signaling molecules. Among them, phosphorylated (p)-NFκB and M-CSF are essential osteoclastogenic factors. Our results indeed showed that both M-CSF and p-NFκB were decreased in CD44 or C1GALT1 knockdown cells (**Fig. 3C**). Taken together, these data suggest that inhibition of C1GALT1 attenuates HA-CD44 signaling through decreased membrane targeting of CD44, which may suppress cancer-induced osteoclastogenesis by downregulating M-CSF and p-NFκB expression.

CD44 is involved in C1GALT1-mediated osteoclastogenesis and mutations in the O-glycosites on the stem region of CD44 abrogate this effect

The analysis of TCGA exon expression data set indicated that CD44v8–10 exons were the most abundant variable exons, and the expression of these three exons was most highly correlated with aggressive phenotypes among breast cancer specimens (25). Moreover, CD44v(3, 8–10) was reported to involve in the formation of invadopodia and the activation of migration processes in metastatic breast cancer cells (36). On the basis of the O-glycosites of CD44 identified by Dr. Henrik Clausen's team, the exon v8–10 region of CD44 variant is highly O-glycosylated (37). However, the biological role of the O-glycosites on the stem region of CD44 has never been reported. We constructed a GalNAc-type O-glycosylation mutant of CD44 with multiple mutations at O-glycosylation sites (Supplementary Fig. S2), and the (Wt) or this mutant (Mu) was expressed in mock or C1GALT1-overexpressing MCF-7 cells, which express low levels of endogenous CD44 and C1GALT1. Western blotting data confirmed the overexpression of C1GALT1, CD44 Wt, and CD44 Mu proteins. We also observed that CD44 Mu exhibited a decreased molecular weight compared with CD44 Wt. Moreover, the expression level of M-

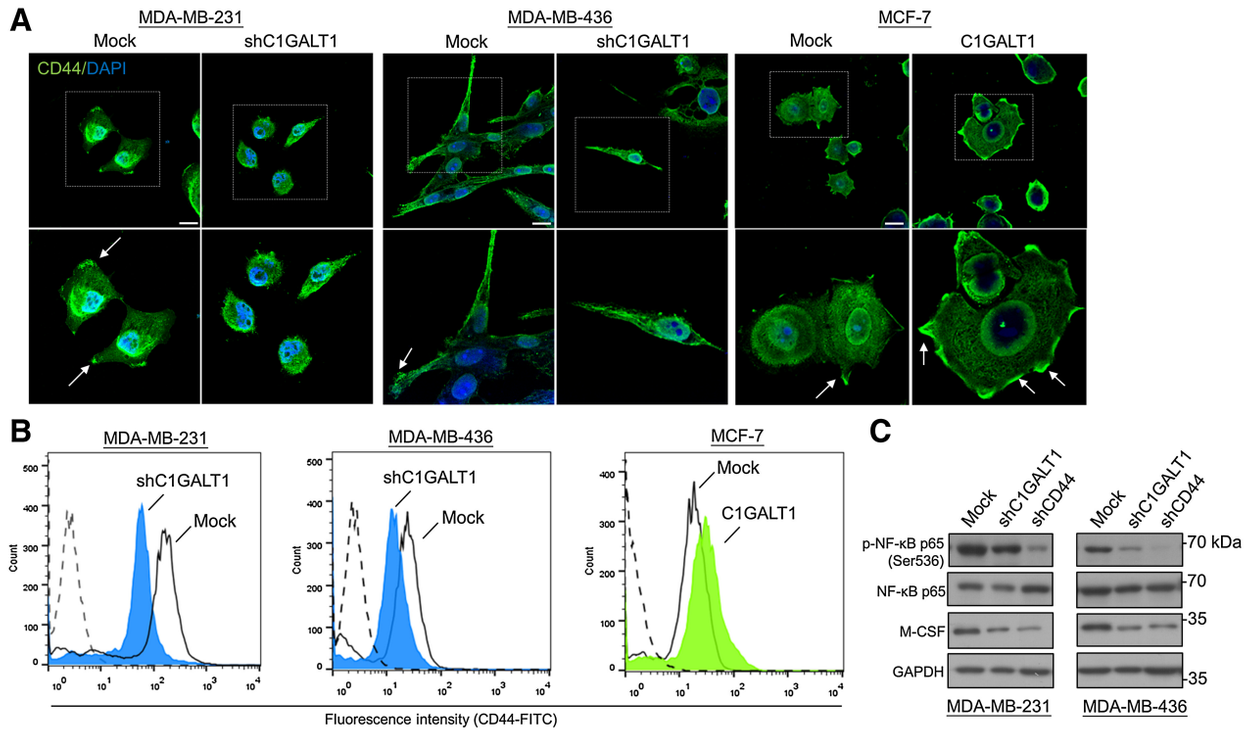

Figure 3.

Impacts of C1GALT1-mediated O-glycans on the surface expression of CD44 and osteoclastogenic signaling. **A,** Representative images showing IF staining of CD44 (green) in C1GALT1 knockdown or overexpressing breast cancer cells. Nuclei were stained with DAPI (blue). Bottom, white arrows indicate focal adhesion-localized CD44. Scale bars, 20 μm ($n = 3$ for each). **B,** Effects of C1GALT1 on the cell surface expression of CD44. Flow cytometry with FITC-CD44 on surfaces of breast cancer cells with C1GALT1 knockdown or overexpression. **C,** Effects of C1GALT1 or CD44 knockdown on the phosphorylation of NF-κB and the expression of M-CSF in breast cancer cells. Representative images of Western blots analyses showing the expression of p-NF-κB, NF-κB, and M-CSF. GAPDH was used as an internal control.

CSF was increased in the C1GALT1/CD44 Wt group but decreased in the CD44 Mu group compared with the C1GALT1 group (**Fig. 4A**). We further performed IF staining to examine the localization of CD44 Wt and CD44 Mu in mock or C1GALT1-overexpressing MCF-7 cells. The results indicated that CD44 Wt was mainly present on the cell surface of C1GALT1-overexpressing cells. In contrast, CD44 Mu was predominantly observed on intracellular vesicles and the Golgi apparatus, and C1GALT1 overexpression enhanced its targeting to the plasma membrane (**Fig. 4B**). The effect of the mutations in O-glycosylation sites on the membrane-targeting of CD44 was further confirmed by the staining of tumor spheres (Supplementary Fig. S3). Furthermore, the tumorsphere size was slightly increased in C1GALT1- and CD44 Wt-expressing cells. We next examined whether blocking the O-glycosylation of CD44 affects HA-binding in breast cancer cells and hampers cancer-mediated osteoclastogenesis. Cell–HA adhesion assays showed that C1GALT1- or CD44 Wt-overexpressing MCF-7 cells increased HA-binding ability compared with control cells, and C1GALT1-expressing cells cotransduced with CD44 Wt increased HA-binding ability compared with their control C1GALT1-expressing cells. However, C1GALT1-expressing cells cotransduced CD44 Mu significantly decreased HA-binding ability compared with C1GALT1-expressing cells cotransduced CD44 Wt. The data indicated that CD44 is involved in C1GALT1-mediated breast cancer cell–binding to HA, and the O-glycosites on the stem region of CD44 have considerable influence on this effect (**Fig. 4C**). Similar correlations were observed in the osteoclastogenesis analysis of human breast cancer cells, showing that C1GALT1- and CD44 Wt-expressing cells induced the most prominent osteoclast differentiation analyzed by TRAP staining (**Fig. 4D**). These results correlated with the protein levels of M-CSF in C1GALT1- and CD44 Wt-expressing cells are higher than those in other groups.

Itraconazole alters O-glycosylation and subcellular localization of CD44 as well as suppresses cell–HA adhesion and osteoclastogenic effects of breast cancer cells

We next aimed to identify a potent compound against breast cancer cell-mediated osteoclastogenesis. Lin and colleagues reported itraconazole as a C1GALT1 inhibitor (20). The results of Western blot analysis confirmed that 2.5 μmol/L itraconazole decreased the protein levels of C1GALT1 and resulted in a molecular weight shift of CD44 (**Fig. 5A**). Moreover, lysates from itraconazole-treated cells were pulled down with VVA lectin, and the results indicated a dramatic increase in truncated O-glycans (Tn antigens) on CD44. IF microscopy also demonstrated that the localization of CD44 in the focal contact was blocked in itraconazole-treated breast cancer cells (**Fig. 5B**). To investigate the effect of itraconazole on the adhesion of breast cancer cells to HA, cell–HA adhesion assays were performed in MDA-MB-231 and MDA-MB-436 cells treated with DMSO solvent control or itraconazole. The results showed that 2.5 μmol/L itraconazole significantly inhibited cell adhesion to immobilized HA in both breast cancer cell lines (**Fig. 5C**). To examine the effect of itraconazole on cancer-mediated osteoclastogenesis, TRAP staining was performed to

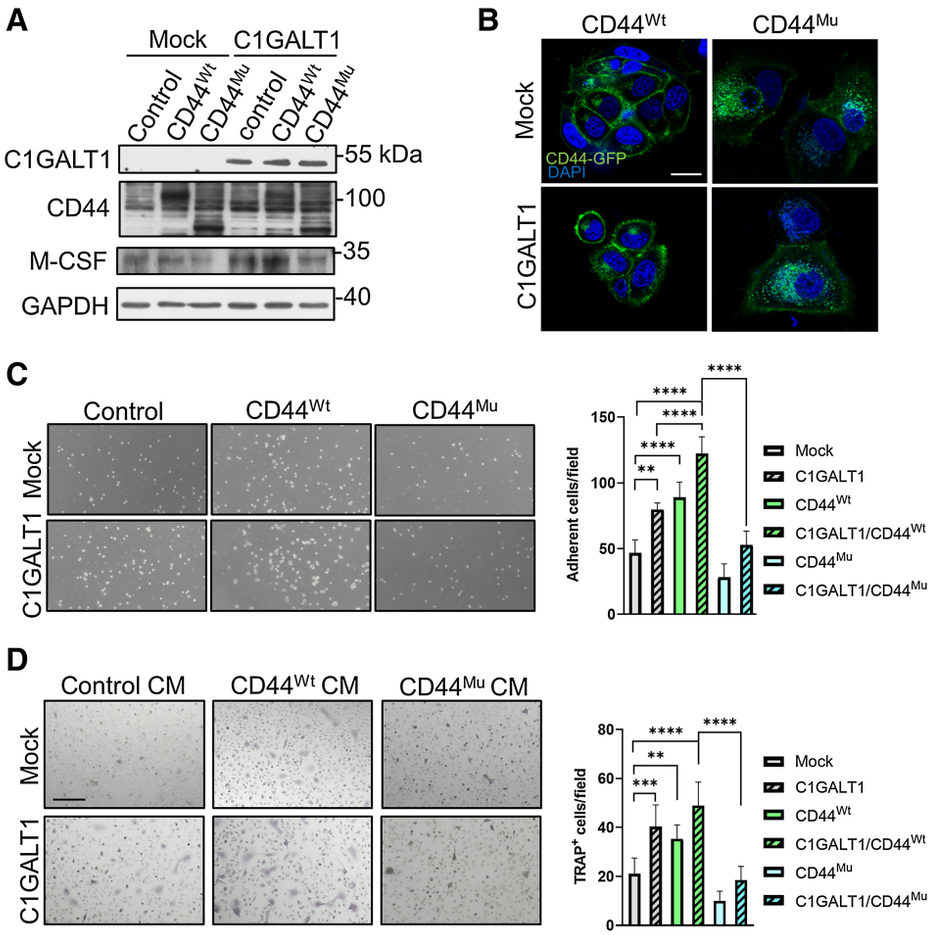

Figure 4.
Site-specific mutations in the O-glycosites on the stem region of CD44 reverse C1GALT1-mediated malignant behaviors in breast cancer cells. **A,** Western blots analyses showing the expression levels of C1GALT1, CD44, and M-CSF in mock or C1GALT1-overexpressing MCF-7 cells infected with control, $CD44^{wt}$, or $CD44^{Mu}$ lentivirus. GAPDH was used as an internal control. **B,** Representative images showing IF staining of CD44 (green) in control (mock) or C1GALT1-overexpressing (C1GALT1) breast cancer cells infected with $CD44^{wt}$ or $CD44^{Mu}$ lentivirus. Nuclei were stained with DAPI (blue). Scale bar, 20 μm ($n = 3$ for each). **C,** Cell–HA adhesion assays. Representative pictures showing breast cancer cells adhered to plates coated with HA. Magnification, 100×. Data are presented as the mean ± SD ($n = 3$). **, $P < 0.01$; ***, $P < 0.001$. **D,** Osteoclast differentiation assays. Representative images showing TRAP staining of *in vitro* differentiated osteoclasts derived from mouse bone marrow cells treated with conditioned medium from mock or C1GALT1-overexpressing MCF-7 cells infected with control, $CD44^{wt}$, or $CD44^{Mu}$ lentivirus. Data are presented as the mean ± SD of TRAP-positive cells ($n = 3$). Scale bars, 100 μm. **, $P < 0.01$; ***, $P < 0.001$; ****, $P < 0.0001$.

stain osteoclasts differentiated from mouse BMMCs treated with the conditioned media of DMSO or itraconazole-treated MDA-MB-231 and MDA-MB-436 cells. The results showed that 2.5 μmol/L itraconazole significantly suppressed cancer-mediated osteoclastogenesis in both breast cancer cell lines (**Fig. 5D**). These results support that downregulation of C1GALT1 by a genetic or pharmaceutical compound in breast cancer cells can suppress cancer cell–induced osteoclastogenesis *in vitro*, that is at least partially mediated through the HA–CD44 signaling pathway.

Knockdown of C1GALT1 ameliorates bone loss from breast cancer–associated bone metastasis *in vivo*

To further explore whether the truncation of O-glycans mediated by silencing C1GALT1 influences breast cancer cell-induced osteolysis in bone metastases *in vivo*, we intracardially injected immune-deficient mice with the same amount of mock or C1GALT1 knockdown MDA-MB-231 cells and performed TRAP staining and micro-CT analysis to analyze osteoclastogenesis and bone density using dissected tibial bones. Image analysis of H&E-stained bone sections showed that C1GALT1 knockdown resulted in fewer MDA-MB-231 cells infiltrating the bone than mock knockdown cells (**Fig. 6A**). In addition, the expression levels of CD44 and M-CSF, breast cancer stem-like cell and osteoclastic markers, respectively, were investigated by IHC staining using serial sections of the tibia. The results showed that CD44 was predominantly observed at the perinuclear region in the tumor nodules of C1GALT1 knockdown MDA-MB-231 cells, which is in line with the findings using C1GALT1 knockdown cells and CD44 Mu *in vitro* (**Fig. 6B**). Moreover, C1GALT1 knockdown decreased M-CSF expression in bone sections. For histomorphometric analysis of bone, the results from histologic TRAP staining and micro-CT analysis indicated less osteoclastogenesis in the tibia of mice injected with C1GALT1 knockdown MDA-MB-231 cells compared with mock knockdown cells (**Fig. 6C** and **D**), as demonstrated by fewer TRAP-positive cells and greater bone microarchitectural parameters, including bone density, trabecular number, and trabecular thickness. These results demonstrated that knockdown of C1GALT1 suppresses the metastasis of breast cancer cells to bone and ameliorates breast cancer cell–induced bone loss, that may be partially mediated through the CD44 signaling pathway.

Discussion

Bone-specific homing and colonization of cancer cells are important features of malignant breast tumors (38). Osteolytic lesions caused by breast cancer cell-mediated osteoclast activation release abundant growth factors for tumor growth (39). Glycosylation is one of the necessary co/posttranslational modifications of proteins. It plays a critical role in determining protein structure, function, and stability. Accumulating evidence indicates that aberrant glycosylation has been linked with a significant contribution in aggressive cancers. Notably,

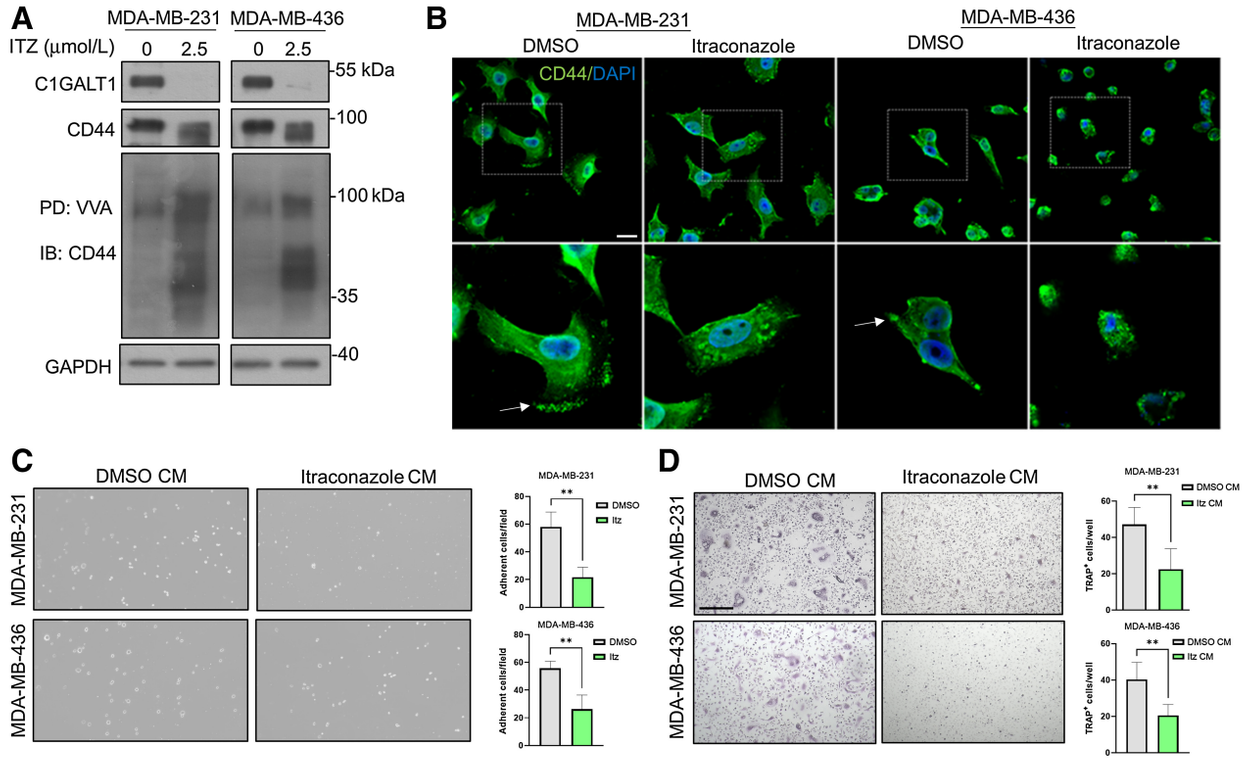

Figure 5.

Itraconazole alters O-glycosylation and subcellular localization of CD44 as well as suppresses cell-HA adhesion and osteoclastogenic effects of breast cancer cells. **A,** Western blots analyses showing the effects of itraconazole on C1GALT1 expression and CD44 O-glycosylation. MDA-MB-231 and MDA-MB-436 cells were treated with DMSO or itraconazole (ITZ) for 48 hours and collected for Western blot analysis of C1GALT1 and CD44. To detect changes in O-glycans on CD44, Tn-decorated proteins in cell lysates were pulled down with VVA-agarose beads for 18 hours and then immunoblotted (IB) with an anti-CD44 antibody. GAPDH was used as an internal control. **B,** Representative images showing IF staining of CD44 (green) in breast cancer cells treated with DMSO or itraconazole. Nuclei were stained with DAPI (blue). Bottom panels: white arrows indicate focal adhesion–localized CD44. Scale bar, 20 μm ($n = 3$ for each). **C,** Cell–HA adhesion assays. Representative pictures showing DMSO- or itraconazole-treated breast cancer cells adhered on plates coated with HA. Magnification, 100×. Data are presented as the mean ± SD ($n = 3$). **, $P < 0.01$. **D,** Osteoclast differentiation assays. Representative images showing TRAP staining of *in vitro* differentiated osteoclasts derived from mouse bone marrow cells treated with conditioned medium from DMSO- or itraconazole-treated breast cancer cells. Data are presented as the mean ± SD of TRAP-positive cells ($n = 3$). Scale bars, 100 μm. **, $P < 0.01$.

Leon and colleagues provided evidence that truncation of O-glycans on CD44 increases cancer stem cell (CSC) activation through increasing NANOG activation (29). However, CD44 is a multifunctional mediator of cancer progression, particularly in breast cancer development and bone metastasis (31). Here, our studies provide an alternative perspective on the essential function of GalNAc-type O-glycans on CD44 in breast cancer cell-induced osteoclastogenesis and bone metastasis. Moreover, HA–CD44 interaction is correlated with more aggressive clinicopathologic features and is associated with poor prognosis in patients with TNBC (31, 40, 41). Our results also found that the effect of C1GALT1 overexpression on malignant cell phenotypes was enhanced and abolished by expressing CD44 Wt and CD44 Mu in C1GALT1-overexpressing breast cancer cells. These results suggest that C1GALT1-mediated CD44 O-glycosylation changes partly regulate the malignant behaviors of breast cancer cells. Furthermore, the analysis of tumor samples from patients with breast cancer indicated that C1GALT1 (core 1 synthase) is significantly upregulated in TNBC and that high C1GALT1 expression is correlated with adverse clinicopathologic features, including lymph node metastasis and the expression of Ki67 and CD44. The results of clinical correlation were supported by *in vitro* findings of high expression of C1GALT1 and CD44 in TNBC cell lines and the positive correlation between C1GALT1 and CD44 expression. Our *in vitro* experiments using VVA lectin pull-down assays confirmed that downregulation of C1GALT1 by genetic silencing or pharmacologic inhibition increased Tn antigens on the breast cancer cell surface. We further pulled down glycoproteins with VVA-agarose beads, followed by MS, to identify CD44 as one of the main C1GALT1-regulated surface glycoproteins (Supplementary Table S1). It has been reported that loss of C1GALT1 may affect O-glycosylation, stability, or degradation of several proteins (21, 42). Indeed, we found that silencing C1GALT1 leads to more Tn antigens on CD44 and impairs its expression at the protein but not mRNA level. To further elucidate the effect of Tn expression on CD44 localization, the results from IF microscopy of membrane permeabilized cells showed that C1GALT1 could regulate the translocation of CD44 to focal adhesion contacts in breast cancer cells. Moreover, silencing C1GALT1 reduced HA-mediated adhesion in breast cancer cells. In contrast, overexpression of C1GALT1 promoted plasma membrane targeting of CD44 and increased cell adhesion to HA. Taken together, this is the first study to demonstrate C1GALT1-mediated O-glycosylation as a critical regulatory factor for CD44 localization and function. These

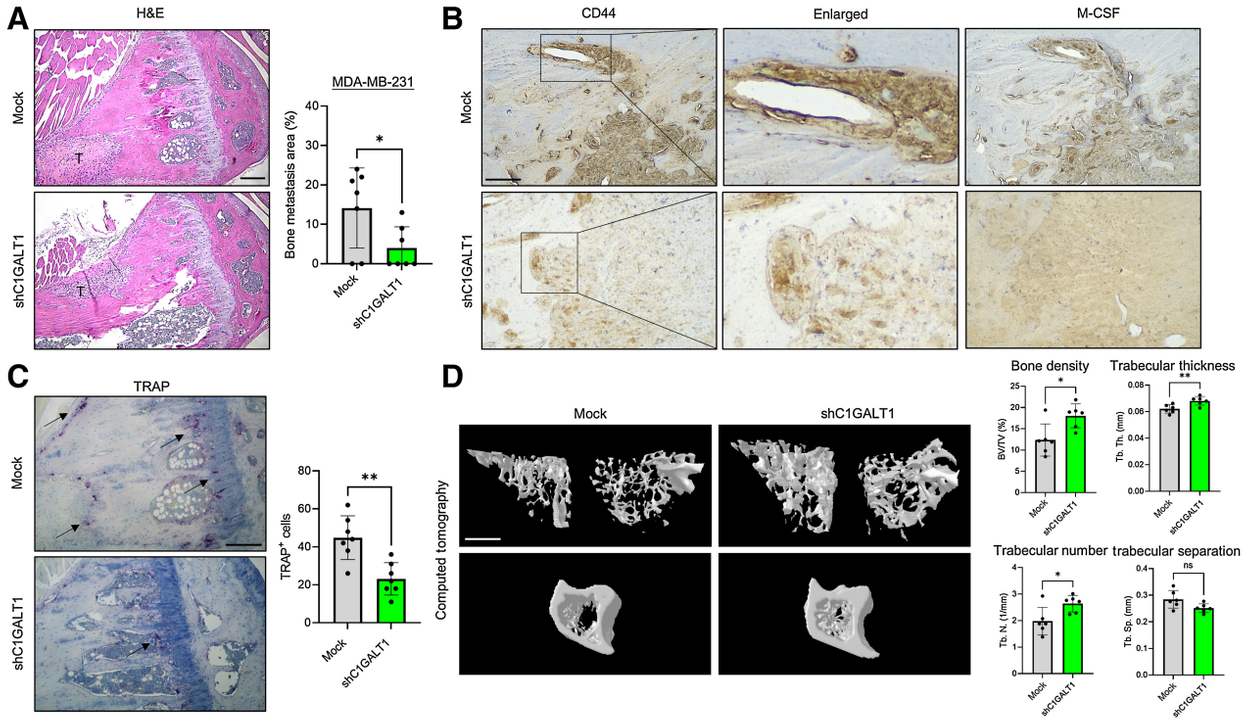

Figure 6.

Knockdown of C1GALT1 ameliorates bone loss from breast cancer–associated bone metastasis *in vivo*. **A,** H&E staining. Representative H&E-stained sections of the tibia from mice injected with mock or shC1GALT1 transfectants. Experimental bone metastasis was induced by intracardiac injection of MDA-MB-231 cells for 60 days. T indicates metastatic tumor. The analysis of the metastatic tumor area was presented in the right. Scale bar = 200 μmol/L. *, $P < 0.05$. **B,** IHC of CD44 and M-CSF. Representative images showing IHC staining of CD44 and M-CSF in the metastatic breast tumor of the bone. Brown colors represent positively stained cells. Scale bar = 50 μmol/L. **C,** TRAP staining. Representative images showing TRAP staining of tibia metastasized with mock or C1GALT1 knockdown MDA-MB-231 cells. Arrows indicate TRAP-positive cells. Scale bars, 100 μm. The statistical analysis for the number of TRAP-positive cells from the sections was shown. **, $P < 0.01$. **D,** Micro-CT analysis. Representative micro-CT images of tibiae from mice injected with mock or shC1GALT1 transfectants. Scale bar, 1 mm. Three-dimensional morphometric analysis of bone parameters: bone volume per tissue trabecular volume (BV/TV); trabecular number (Tb. N.); trabecular thickness (Tb. Th.); trabecular separation (Tb. Sp.). $n = 7$ per group; *, $P < 0.05$; **, $P < 0.01$; ns, not significant.

findings support the concept that changes in the glycosylation of CD44 have profound effects on its interaction with HA (32).

CD44 variant (v) isoforms, designated CD44v1–10, have been shown to promote malignant cancer phenotypes (43, 44), including an increase in osteoclastogenesis and bone metastasis (31, 45), especially CD44v8–10. Most of the MS-identified O-glycosites are located in the stem region of CD44v (37). However, the function of O-glycosylation on the stem region of CD44v has not yet been elucidated. In this study, we showed that loss of GalNAc-type O-glycans on the stem region of CD44v8–10 leads to substantial Golgi retention. The impairment of cell surface expression explains why CD44 Mu cannot mediate cell–HA adhesion. Supportively, C1GALT1 overexpression significantly enhanced the plasma membrane localization of CD44 Wt. Consistent with our findings, previous reports have identified the essential function of O-glycans at the stem region for the efficient Golgi export of Tac (IL2 receptor α subunit) and low-density lipoprotein receptor (46, 47). Moreover, it has been reported that O-glycans at serine–glycine motifs localized in the membrane-proximal ectodomain of CD44 are indispensable for CD44 shedding, which is a critical step in the regulation of CD44-dependent migration and invasion (48, 49). These results suggest that CD44v requires the O-glycosylation at its juxtamembrane region for its postGolgi trafficking to the plasma membrane.

After the binding of HA, CD44 receptors activate various intracellular signaling molecules, such as ERK, PI3K, and NFκB, leading to M-CSF production to promote cell migration, invasion, and distant metastasis (50–53). Indeed, our data showed that C1GALT1 knockdown decreased phospho-NFκB and M-CSF levels in breast cancer cells. IHC staining of the tibia in our mouse model of bone metastasis also demonstrated the reduced expression of M-CSF by C1GALT1 knockdown. Furthermore, CD44 Wt but not CD44 Mu elevated M-CSF levels in MCF-7 cells overexpressing C1GALT1. These results suggest a critical role of GalNAc-type O-glycans in the HA–CD44 signaling axis and targeting the O-glycans on CD44 as a potential therapeutic strategy for blocking cancer bone metastasis.

Authors' Disclosures

C. Kuo reports grants from National Science and Technology Council, ROC during the conduct of the study; grants from National Science and Technology Council, ROC and grants from National Health Research Institutes outside the submitted work. No disclosures were reported by the other authors.

Authors' Contributions

N.-Y. Lin: Supervision, funding acquisition, writing–original draft, project administration. **J.-J. Lee:** Resources, data curation, funding acquisition. **S.-T. Chen:** Software, visualization. **J.-A. Lin:** Investigation. **C.-H. Lin:** Investigation. **H.-Y. Lin:**

Investigation, visualization. **Y.-H. Su:** Investigation, visualization. **C.-C. Chen:** Methodology, writing–review and editing. **M.-C. Lin:** Conceptualization, methodology, writing–review and editing. **C.-Y. Kuo:** Conceptualization, writing–review and editing. **M.-C. Haung:** Conceptualization, supervision, writing–review and editing.

Acknowledgments

We thank Ru-Xuan Zheng, Ya-Wen Hung, Yong-Xun Xiao, and Yi-Zhen Wu for their excellent technical assistance. We would like to acknowledge the service provided by the flow cytometric analysis and image acquisition and analysis of the First Core Laboratory, National Taiwan University College of Medicine. This study was supported by the Excellent Translational Medicine Research Projects of National Taiwan University College of Medicine and National Taiwan University Hospital: 107C101-B3, 108C101–83, 109C101–93, NSCCMOH-94–8 and NSCCMOH-131–92 (to N.-Y. Lin) and Ministry of Science and Technology, R.O.C. 106–2320-B-002–004-MY3 (to N.-Y. Lin), and 109–2320-B-002 -039 (to N.-Y. Lin).

The publication costs of this article were defrayed in part by the payment of publication fees. Therefore, and solely to indicate this fact, this article is hereby marked "advertisement" in accordance with 18 USC section 1734.

Note

Supplementary data for this article are available at Molecular Cancer Research Online (http://mcr.aacrjournals.org/).

Received November 14, 2022; revised February 13, 2023; accepted April 6, 2023; published first April 11, 2023.

References

1. Selvaggi G, Scagliotti GV. Management of bone metastases in cancer: a review. Crit Rev Oncol Hematol 2005;56:365–78.
2. Chen YC, Sosnoski DM, Mastro AM. Breast cancer metastasis to the bone: mechanisms of bone loss. Breast Cancer Res 2010;12:215.
3. Mancino AT, Klimberg VS, Yamamoto M, Manolagas SC, Abe E. Breast cancer increases osteoclastogenesis by secreting M-CSF and upregulating RANKL in stromal cells. J Surg Res 2001;100:18–24.
4. Ney JT, Fehm T, Juhasz-Boess I, Solomayer EF. RANK, RANKL and OPG expression in breast cancer - influence on osseous metastasis. Geburtshilfe Frauenheilkd 2012;72:385–91.
5. Blair HC, Robinson LJ, Zaidi M. Osteoclast signalling pathways. Biochem Biophys Res Commun 2005;328:728–38.
6. Kogan M, Haine V, Ke Y, Wigdahl B, Fischer-Smith T, Rappaport J. Macrophage colony stimulating factor regulation by nuclear factor kappa B: a relevant pathway in human immunodeficiency virus type 1 infected macrophages. DNA Cell Biol 2012;31:280–9.
7. Ara T, Declerck YA. Interleukin-6 in bone metastasis and cancer progression. Eur J Cancer 2010;46:1223–31.
8. Tulotta C, Ottewell P. The role of IL-1B in breast cancer bone metastasis. Endocr Relat Cancer 2018;25:R421–34.
9. Hiraga T, Ito S, Nakamura H. Cancer stem-like cell marker CD44 promotes bone metastases by enhancing tumorigenicity, cell motility, and hyaluronan production. Cancer Res 2013;73:4112–22.
10. Ide H, Hatake K, Terado Y, Tsukino H, Okegawa T, Nutahara K, et al. Serum level of macrophage colony-stimulating factor is increased in prostate cancer patients with bone metastasis. Hum Cell 2008;21:1–6.
11. Kolbl AC, Jeschke U, Friese K, Andergassen U. The role of TF- and Tn-antigens in breast cancer metastasis. Histol Histopathol 2016;31:613–21.
12. Tarp MA, Clausen H. Mucin-type O-glycosylation and its potential use in drug and vaccine development. Biochim Biophys Acta 2008;1780:546–63.
13. Karacosta LG, Fisk JC, Jessee J, Tati S, Turner B, Ghazal D, et al. Preclinical analysis of JAA-F11, a specific anti-thomsen-friedenreich antibody via immunohistochemistry and in vivo imaging. Transl Oncol 2018;11:450–66.
14. Schindlbeck C, Jeschke U, Schulze S, Karsten U, Janni W, Rack B, et al. Characterisation of disseminated tumor cells in the bone marrow of breast cancer patients by the Thomsen-Friedenreich tumor antigen. Histochem Cell Biol 2005;123:631–7.
15. Wu YM, Liu CH, Huang MJ, Lai HS, Lee PH, Hu RH, et al. C1GALT1 enhances proliferation of hepatocellular carcinoma cells via modulating MET glycosylation and dimerization. Cancer Res 2013;73:5580–90.
16. Hung JS, Huang J, Lin YC, Huang MJ, Lee PH, Lai HS, et al. C1GALT1 overexpression promotes the invasive behavior of colon cancer cells through modifying O-glycosylation of FGFR2. Oncotarget 2014;5:2096–106.
17. Tzeng SF, Tsai CH, Chao TK, Chou YC, Yang YC, Tsai MH, et al. O-Glycosylation-mediated signaling circuit drives metastatic castration-resistant prostate cancer. FASEB J 2018:fj201800687.
18. Lee PC, Chen ST, Kuo TC, Lin TC, Lin MC, Huang J, et al. C1GALT1 is associated with poor survival and promotes soluble Ephrin A1-mediated cell migration through activation of EPHA2 in gastric cancer. Oncogene 2020;39:2724–40.
19. Chou CH, Huang MJ, Chen CH, Shyu MK, Huang J, Hung JS, et al. Up-regulation of C1GALT1 promotes breast cancer cell growth through MUC1-C signaling pathway. Oncotarget 2015;6:6123–35.
20. Lin MC, Chien PH, Wu HY, Chen ST, Juan HF, Lou PJ, et al. C1GALT1 predicts poor prognosis and is a potential therapeutic target in head and neck cancer. Oncogene 2018;37:5780–93.
21. Du T, Jia X, Dong X, Ru X, Li L, Wang Y, et al. Cosmc disruption-mediated aberrant O-glycosylation suppresses breast cancer cell growth via impairment of CD44. Cancer Manag Res 2020;12:511–22.
22. Shao B, Yago T, Setiadi H, Wang Y, Mehta-D'souza P, Fu J, et al. O-glycans direct selectin ligands to lipid rafts on leukocytes. Proc Natl Acad Sci U S A 2015;112:8661–6.
23. Brown RL, Reinke LM, Damerow MS, Perez D, Chodosh LA, Yang J, et al. CD44 splice isoform switching in human and mouse epithelium is essential for epithelial-mesenchymal transition and breast cancer progression. J Clin Invest 2011;121:1064–74.
24. Dalerba P, Dylla SJ, Park IK, Liu R, Wang X, Cho RW, et al. Phenotypic characterization of human colorectal cancer stem cells. Proc Natl Acad Sci U S A 2007;104:10158–63.
25. Zhang H, Brown RL, Wei Y, Zhao P, Liu S, Liu X, et al. CD44 splice isoform switching determines breast cancer stem cell state. Genes Dev 2019;33:166–79.
26. Chen C, Zhao S, Karnad A, Freeman JW. The biology and role of CD44 in cancer progression: therapeutic implications. J Hematol Oncol 2018;11:64.
27. Senbanjo LT, Chellaiah MA. CD44: a multifunctional cell surface adhesion receptor is a regulator of progression and metastasis of cancer cells. Front Cell Dev Biol 2017;5:18.
28. Skelton TP, Zeng C, Nocks A, Stamenkovic I. Glycosylation provides both stimulatory and inhibitory effects on cell surface and soluble CD44 binding to hyaluronan. J Cell Biol 1998;140:431–46.
29. Leon F, Seshacharyulu P, Nimmakayala RK, Chugh S, Karmakar S, Nallasamy P, et al. Reduction in O-glycome induces differentially glycosylated CD44 to promote stemness and metastasis in pancreatic cancer. Oncogene 2022;41:57–71.
30. Afkari H, Makrufardi F, Hidayat B, Budiawan H, Sundawa Kartamihardja AH. Correlation between ER, PR, HER-2, and Ki-67 with the risk of bone metastases detected by bone scintigraphy in breast cancer patients: A cross sectional study. Ann Med Surg (Lond) 2021;67:102532.
31. McFarlane S, Coulter JA, Tibbits P, O'Grady A, McFarlane C, Montgomery N, et al. CD44 increases the efficiency of distant metastasis of breast cancer. Oncotarget 2015;6:11465–76.
32. Bartolazzi A, Nocks A, Aruffo A, Spring F, Stamenkovic I. Glycosylation of CD44 is implicated in CD44-mediated cell adhesion to hyaluronan. J Cell Biol 1996;132:1199–208.
33. Vuorio J, Skerlova J, Fabry M, Veverka V, Vattulainen I, Rezacova P, et al. N-Glycosylation can selectively block or foster different receptor-ligand binding modes. Sci Rep 2021;11:5239.
34. Azevedo R, Gaiteiro C, Peixoto A, Relvas-Santos M, Lima L, Santos LL, et al. CD44 glycoprotein in cancer: a molecular conundrum hampering clinical applications. Clin Proteomics 2018;15:22.
35. Lin NY, Chen ST, Chang HL, Lu MY, Yang YL, Chou SW, et al. C1GALT1 expression predicts a favorable prognosis and suppresses malignant phenotypes via TrkA signaling in neuroblastoma. Oncogenesis 2022;11:8.

36. Bourguignon LY, Gunja-Smith Z, Iida N, Zhu HB, Young LJ, Muller WJ, et al. CD44v(3,8–10) is involved in cytoskeleton-mediated tumor cell migration and matrix metalloproteinase (MMP-9) association in metastatic breast cancer cells. J Cell Physiol 1998;176:206–15.
37. Steentoft C, Vakhrushev SY, Joshi HJ, Kong Y, Vester-Christensen MB, Schjoldager KT, et al. Precision mapping of the human O-GalNAc glycoproteome through SimpleCell technology. EMBO J 2013;32:1478–88.
38. Akhtari M, Mansuri J, Newman KA, Guise TM, Seth P. Biology of breast cancer bone metastasis. Cancer Biol Ther 2008;7:3–9.
39. Langley RR, Fidler IJ. The seed and soil hypothesis revisited–the role of tumor-stroma interactions in metastasis to different organs. Int J Cancer 2011;128: 2527–35.
40. Zou W, Yang Y, Zheng R, Wang Z, Zeng H, Chen Z, et al. Association of CD44 and CD24 phenotype with lymph node metastasis and survival in triple-negative breast cancer. Int J Clin Exp Pathol 2020;13:1008–16.
41. Hill A, McFarlane S, Johnston PG, Waugh DJ. The emerging role of CD44 in regulating skeletal micrometastasis. Cancer Lett 2006;237:1–9.
42. Campos D, Freitas D, Gomes J, Magalhaes A, Steentoft C, Gomes C, et al. Probing the O-glycoproteome of gastric cancer cell lines for biomarker discovery. Mol Cell Proteomics 2015;14:1616–29.
43. Toole BP. Hyaluronan promotes the malignant phenotype. Glycobiology 2002; 12:37R–42R.
44. Wang L, Zuo X, Xie K, Wei D. The role of CD44 and cancer stem cells. Methods Mol Biol 2018;1692:31–42.
45. Fontanella RA, Sideri S, Di Stefano C, Catizone A, Di Agostino S, Angelini DF, et al. CD44v8–10 is a marker for malignant traits and a potential driver of bone metastasis in a subpopulation of prostate cancer cells. Cancer Biol Med 2021;18: 788–807.
46. Kozarsky K, Kingsley D, Krieger M. Use of a mutant cell line to study the kinetics and function of O-linked glycosylation of low density lipoprotein receptors. Proc Natl Acad Sci U S A 1988;85:4335–9.
47. Sun X, Tie HC, Chen B, Lu L. Glycans function as a Golgi export signal to promote the constitutive exocytic trafficking. J Biol Chem 2020;295:14750–62.
48. Gasbarri A, Del Prete F, Girnita L, Martegani MP, Natali PG, Bartolazzi A. CD44s adhesive function spontaneous and PMA-inducible CD44 cleavage are regulated at post-translational level in cells of melanocytic lineage. Melanoma Res 2003;13: 325–37.
49. Stamenkovic I, Yu Q. Shedding light on proteolytic cleavage of CD44: the responsible sheddase and functional significance of shedding. J Invest Dermatol 2009;129:1321–4.
50. Misra S, Hascall VC, Markwald RR, Ghatak S. Interactions between hyaluronan and its receptors (CD44, RHAMM) regulate the activities of inflammation and cancer. Front Immunol 2015;6:201.
51. Al-Mansoob M, Gupta I, Stefan Rusyniak R, Ouhtit A. KYNU, a novel potential target that underpins CD44-promoted breast tumour cell invasion. J Cell Mol Med 2021;25:2309–14.
52. Herishanu Y, Gibellini F, Njuguna N, Hazan-Halevy I, Farooqui M, Bern S, et al. Activation of CD44, a receptor for extracellular matrix components, protects chronic lymphocytic leukemia cells from spontaneous and drug induced apoptosis through MCL-1. Leuk Lymphoma 2011;52:1758–69.
53. Lu X, Yang R, Zhang L, Xi Y, Zhao J, Wang F, et al. Macrophage colony-stimulating factor mediates the recruitment of macrophages in triple negative breast cancer. Int J Biol Sci 2019;15:2859–71.